6.3 SIMULATED CONVECTIVE LINES WITH PARALLEL PRECIPITATION

Matthew D. Parker*
University of Nebraska–Lincoln, Lincoln, Nebraska

1. INTRODUCTION AND BACKGROUND

Mesoscale convective systems (MCSs) are known to impact civilization by frequently producing severe weather (large hail, tornadoes and other damaging winds, and flash flooding). Indeed, Doswell et al. (1996) reported that a large fraction of flash floods are attributable to MCSs, and Schumacher (2003) confirmed their importance in his study of "extreme rain events". As explained by Doswell et al. (1996), the total point rainfall produced by a precipitation system is a function not only of the precipitation rate, but also of the system's arrangement of convective and stratiform precipitation elements, and the system's overall motion vector.

Toward this end, Parker and Johnson (2000, herafter PJ00) studied the organization of linear MCSs (that is, MCSs that contained a convective line) in the central United States, and found that there were three distinct horizontal reflectivity archetypes (Fig. 1), each of which had a unique arrangement of convective and stratiform precipitation and a unique motion speed. The well–known convective line with trailing stratiform (TS) precipitation mode composed approximately 60% of the PJ00 study population, and has heretofore been widely studied. However, a surprising result was that roughly 20% of the studied systems were best described by the convective line with leading stratiform (LS) precipitation archetype, and that roughly 20% were best described by the convective line with parallel stratiform (PS) precipitation archetype.

Recent studies have addressed some elements of the dynamics, structures, and maintenance of LS MCSs. However, to this point PS MCSs appear to have received little, if any, detailed attention as a kinematically and dynamically unique convective mode. As discussed by PJ00 and Schumacher (2003), PS MCSs often evince line–parallel training of convective echoes such that, in slow–moving cases, they are conducive to tremendous local rainfall totals. A greater understanding of PS MCSs will likely contribute to improvements in the forecasting and warning of hazardous weather, and to deeper insight into the processes that govern all convective systems. As an initial step in that direction, the present study considers idealized simulations of convective lines with parallel precipitation.

* *Corresponding author address:* Matthew D. Parker, Department of Geosciences, University of Nebraska–Lincoln, 214 Bessey Hall, Lincoln, NE 68588–0340. E-mail: parker@updraft.unl.edu

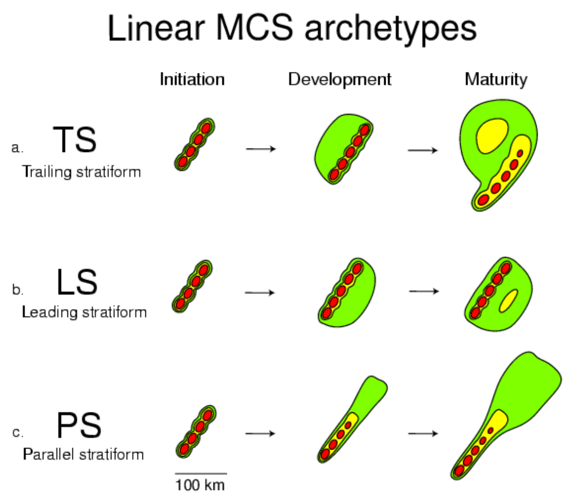

Figure 1: Schematic reflectivity drawing of idealized life cycles for three linear MCS archetypes from Parker and Johnson (2000): (a) leading line trailing stratiform (TS), (b) convective line with leading stratiform (LS), (c) convective line with parallel stratiform (PS). Approximate time interval between phases: for TS 3–4 h; for LS 2–3 h; for PS 2–3 h. Levels of shading roughly correspond to 20, 40, and 50 dBZ.

2. METHOD

This work incorporated 3D simulations using version 5.1.0 of the Advanced Regional Prediction System (ARPS), a fully compressible nonhydrostatic model (Xue et al., 2000, 2001). In order to explicitly simulate convective clouds on the 600x600x20 km domain, the simulations had horizontal grid spacings of 1 km, with an averaged vertical grid spacing of 400 m, ranging from 200 m in the lowest 2 km of the domain to 625 m in the stratosphere. The basic model configuration was generally that used by Parker and Johnson (2004c); please contact the author for more detail. In order to initiate convection the model included a 200 km long, north–south linear warm bubble (+3 K) with random temperature perturbations; this was a simple way to ensure that the initial convection in the model was linear, and was properly oriented with respect to the base state wind profile.

The initial sounding was the idealized Parker and Johnson (2004c) midlatitude MCS sounding, using a smoothed storm–relative wind profile derived from an average of 4 archetypal PS MCS cases from the original PJ00 dataset ("control" in Fig. 2). A battery of sensitivity tests involved isolating all of the control sounding's line–perpendicular (i.e. u–wind) shear to the 0–3 km layer, and all of the line–parallel (i.e. v–wind) shear to the 3–10 km layer (the "compartmentalized shear", or "CS", profile; Fig. 2). The values for the line–perpendicular (u) and line–parallel (v) shear were then each alternately increased and decreased by 50% in the CS profile (CS–1.5xU_s, CS–0.5xU_s, CS–1.5xV_s, CS–0.5xV_s; Fig. 2), in order to test the importance of each component.

3. BASIC THEORY

The pressure perturbation can be decomposed as:

$$p' = p'_B + p'_D \tag{1}$$

wherein p'_B is the component due to buoyancy and p'_{DL} is the component due to dynamic effects. For the anelastic set (also neglecting Coriolis and frictional accelerations), the diagnostic equations for these pressure components in 2D are:

$$\nabla^2 p'_B = \frac{\partial}{\partial z}\left(\rho_o B\right); \tag{2}$$

$$\begin{aligned}\nabla^2 p'_D &= -\rho_o\left[\left(\frac{\partial u}{\partial x}\right)^2 + \left(\frac{\partial v}{\partial y}\right)^2 + \left(\frac{\partial w}{\partial z}\right)^2\right] \\ &\quad +\rho_o\left[w^2\frac{\partial^2}{\partial z^2}\left(\ln\rho_o\right)\right] \\ &\quad -2\rho_o\left(\frac{\partial v}{\partial x}\frac{\partial u}{\partial y} + \frac{\partial u}{\partial z}\frac{\partial w}{\partial x} + \frac{\partial v}{\partial z}\frac{\partial w}{\partial y}\right).\end{aligned} \tag{3}$$

wherein $B \equiv -g\rho'/\rho_o$ is buoyancy, and other variables have their conventional meanings. For the purposes of the following discussion, it is most notable that p'_B is minimized beneath regions of positive buoyancy; in this respect it is not unlike the hydrostatic pressure field. Also for the purposes of the following discussion, it is most notable that p'_D is maximized on the upshear side of an updraft in vertical wind shear, and is minimized on the downshear side. Hence, air parcels in updrafts experience downshear accelerations. Although there are numerous other ways in which atmospheric phenomena

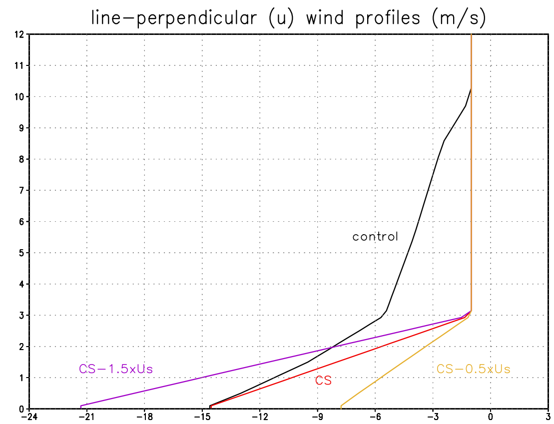

(a)

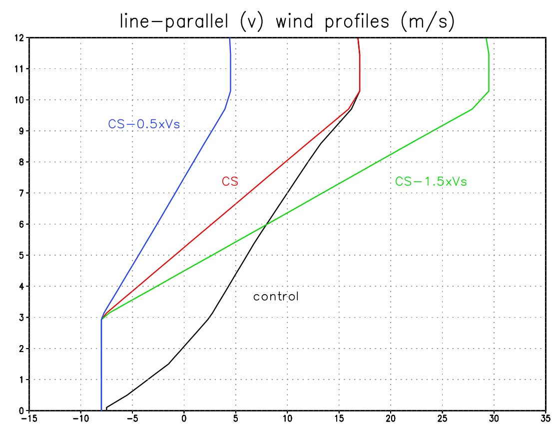

(b)

Figure 2: Wind profiles utilized in the numerical experiments. (a) Line–perpendicular winds (u, m/s). Note that the CS–1.5xV_s and CS–0.5xV_s runs used the CS u–wind profile. (b) Line–parallel winds (v, m/s). Note that the CS–1.5xU_s and CS–0.5xU_s runs used the CS v–wind profile. The vertical axis labels have units of km.

may contribute to pressure perturbations, for simplicity only the "quasi–static" and "updraft in shear" contributions will be discussed at length in this paper.

4. RESULTS

4.1 Control run

The initial line thermal extended from y=200–400 km and, after one hour, the convective cells extended roughly from y=230–370 km (Fig. 3). The line ends were not sites for continuing convective redevelopment during the early part of the simulation because the pool of cold outflow was weaker and shallower there (not shown). At this time, the system was roughly stationary, such that the total wind fields were approximately storm–relative. The basic features of the system's early evolution were that that cold pool expanded southward and westward (Fig. 3a), consistent with low–level storm–relative northeasterlies (Fig. 3b), and that a line–parallel stratiform region began to develop aloft (Fig. 3a), consistent with upper–level storm–relative southerlies (Fig. 3b). Owing to these general behaviors, the simulated PS system exhibits two of the primary features noted in real–world PS systems by PJ00: the convective line backbuilds in a system–relative sense (toward the south in Fig. 3a) as the cold pool expands, and hydrometeors, including cores of heavy precipitation, are observed to move along the line in the opposite sense (toward the north in Fig. 3a). In an environment with significant line–parallel shear, the two behaviors appear to go hand–in–hand, and they continue throughout the simulated PS organizational phase.

In order for a convective system to create a line–parallel precipitation region, there must be along–line flow in the zone of enhanced total water content. In other words, the flow field *within* the convective line of a PS MCS must be line–parallel (e.g., Fig. 3b). An important result is that the along–line flow in the upper troposphere within the convective line is much weaker at t=1 h than the along line flow in the environment (Fig. 3b). Even so, the mean flow above 7 km AGL within the convective plume (x≈270–290 km) has negligible line–perpendicular velocity, such that hydrometeors are largely being advected along the line, despite the diminished line–parallel flow. Because the system's own unique winds are important, the dynamical means of producing these flows require attention.

The along–line wind component reveals cellular structure (not shown), but its decrease is consistent along the entire length of the convective line. The v–wind values in the upper troposphere within the convective line are nearly constant from 4 to 11 km AGL (Fig. 3b), revealing that there is little net line–parallel acceleration of the flow within this layer, and that most of the downs-

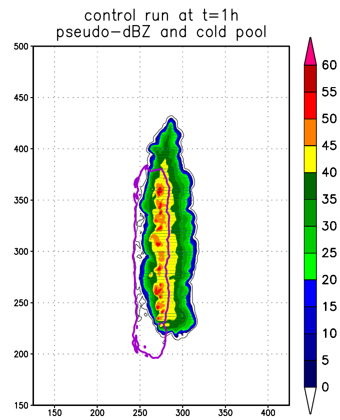

(a)

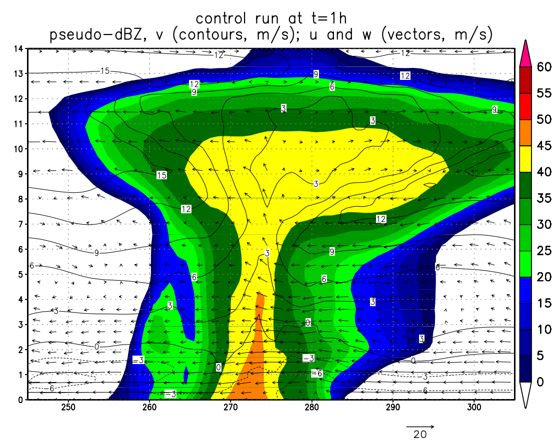

(b)

Figure 3: Output for control PS MCS simulation at t=1h. (a) Plan view of vertically averaged (from z=0–10 km) radar reflectivity (simulated), shaded, with cloud outline plotted as thin black contour (isopleth of $q_{hydro} = 1 \times 10^{-3}$ g/kg) and cold pool outline plotted as thick purple contour (isopleth of θ'=–2K). (b) Vertical cross section of along–line averaged (from y=250–350 km) radar reflectivity (simulated), shaded, line–parallel wind (v, contoured, m/s) and line–perpendicular circulation (u and w, vectors, m/s). All axis labels have units of km.

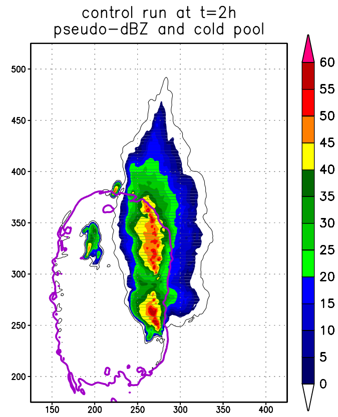

(a)

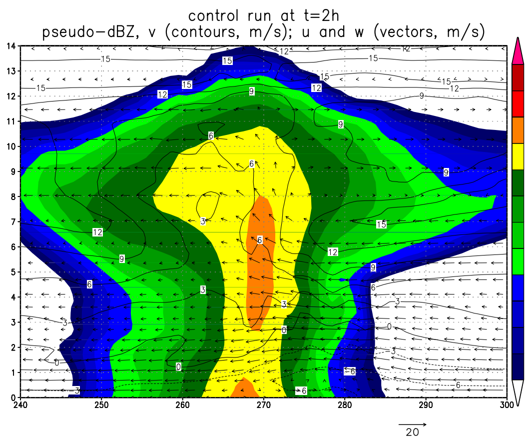

(b)

Figure 4: Same as Fig. 3 but for control PS MCS simulation at t=2h.

hear, along–line dynamic pressure gradient accelerations for updraft air parcels must occur in the lowest 4 km or so AGL. Hence, the PS system diminishes the line–parallel shear in its immediate vicinity. This is consistent with the findings of LeMone (1983) that vertical transports of line–parallel momentum in convective systems are generally downgradient.

By t=2h, it is clear that a line–parallel region of precipitation is developing toward the north (Fig. 4a) as a result of the downshear accelerations imposed on air processed in the convective updrafts. The convective line also appears to have slightly favored the production of leading precipitation over trailing precipitation prior to this time (Figs. 3b and 4a). This results from two facts. Firstly, the lower tropospheric shear vector has a significant rear–to–fore component (Fig. 2a), which is important to the development of line–leading precipitation as discussed by Parker and Johnson (2004a,b,c). And secondly, the lower tropospheric cold pool has not yet increased to its mature strength. The cold pool at this time has an along–line averaged temperature deficit of –6K, and is about 500 m deep (not shown). Even so, by this time the early stages of a mean, rearward–sloping updraft have started to become apparent (Fig. 4b), even as air also continues to flow forward in the overturning updraft (east of x=270 km in Fig. 4b). Much like the front–fed LS systems simulated by Parker and Johnson (2004a), the heaviest precipitation is aft of the surface outflow boundary. Updraft air drops much of its heavy precipitation during the rearward portion of its ascent, before feeding hydrometeors to the parallel, leading, and trailing anvils.

As the system begins to mature by t=3 h, the cold pool strength has increased, with an along–line averaged temperature deficit of approximately –9K, and increasing depth (not shown). By this time, the system has the look of a mature PS MCS, with a long line and a region of line–parallel precipitation extending roughly 50–75 km past the end of the convective line (Fig. 5a). The convective line has also begun to exhibit trailing precipitation in addition to the small leading precipitation region that it developed previously. In part this may be attributable to the onset of weak eastward motion of the convective line, which has progressed roughly 10 km eastward over the past hour owing to the strengthened cold pool. However, following the arguments of Parker and Johnson (2004c, among many others) the intensification of the cold pool is also a significant factor in terms of the strongly rearward accelerations that it produces upon air parcels that it lifts. At this time, most of the mass processed through the convective region exits toward the line–trailing side, and comparatively very little exits the line–leading side (Fig. 5b).

Because their hydrometeors move along the convective line, by their nature PS systems tend to drop most of their precipitation in very close proximity to their outflow boundaries. Hence, their cold pools can intensify quite rapidly. As the surface cold pool gains strength over time, inflowing air parcels begin to experience diminishing eastward accelerations in the convective region, such that even as they are being accelerated downshear in the line–parallel direction, they are also moving strongly rearward. Once the updrafts become rearward–tilted, the system becomes strongly TS in character, in part because of the positive feedbacks associated with the middle–upper tropospheric buoyancy field behind the convective line, its associated quasi–static pressure minimum, and the resulting increasingly rearward pressure gradient accelerations (Szeto and Cho, 1994; Parker and Johnson, 2004b).

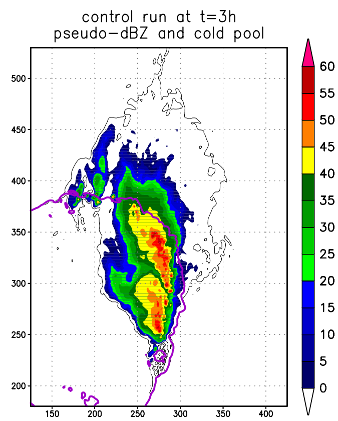

(a)

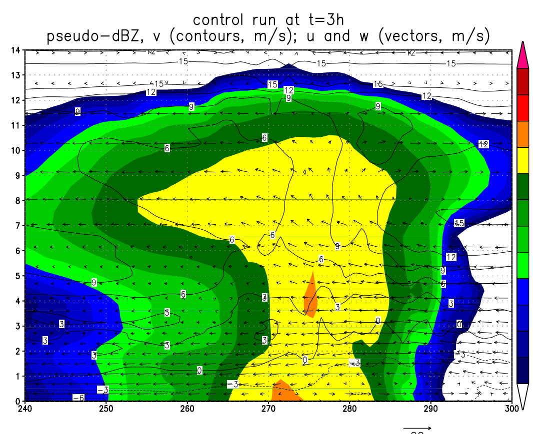

(b)

Figure 5: Same as Fig. 3 but for control PS MCS simulation at t=3h.

A worthwhile question is whether the developing PS region produces a similar feedback and can help to strengthen the along–line accelerations through the buoyant pressure field. The primary problem with this possible mechanism in the PS case is that the stratiform region is not proximate to much of the convective line, such that most of the inflowing air parcels processed by the system do not feel its effects. Instead, the dynamics in the PS system's convective line are quite local, and the mesoscale organization of the system has a comparatively small impact with respect to the TS and LS systems, in which the buoyancy field associated with the trailing or leading cloud is immediately adjacent to the convective line.

When averaged over the entire convective region, the along–line buoyant pressure gradient accelerations seem to be quite significant, but this result is misleading. Analysis of the covariance of vertical velocity with the along–line pressure gradient reveals that, at any time, the buoyant (quasi–static) part of the pressure field never accounts for more than 10.5% of the total covariance, whereas the dynamic (updraft in shear) part of the pressure field always accounts for at least 89.5% of it. In other words, active updrafts are experiencing northward accelerations owing to the line–parallel shear (blue features in Fig. 6). Meanwhile, the air in between the active updrafts, in which the pressure gradient acceleration is southward, is less relevant to the PS structure because it is not fluxing significant total water content upward. Each individual updraft trajectory experiences significant downshear accelerations, but this signal is largely lost when a mesoscale average is performed because the small–scale, transient features that account for them are removed (or cancel one another, e.g. blue features in Fig. 6). In that case, only the weak along–line pressure gradient due to the parallel anvil's buoyancy remains (red features in Fig. 6). Much as for the LS systems discussed by Parker and Johnson (2004a), the mean fields in PS systems do not accurately reflect the transient behavior of the updrafts.

As previously mentioned, the upper tropospheric along–line flow within the convective region is slower than that of the environment at a comparable level. Indeed, as time goes on in the life cycle of the system, the upper level line–parallel flow within the system is decelerated over a continually broadening area. Therefore, the existence of the PS structure does not necessarily seem to favor the continual generation of along–line parcel accelerations. Over the course of time, as the cold pool strengthens and as the along–line shear weakens within the convective line, this may hasten the demise of the PS structure and lead to evolution toward the TS archetype. Given all of the above, it is therefore interesting that MCSs in nature are able to maintain the PS

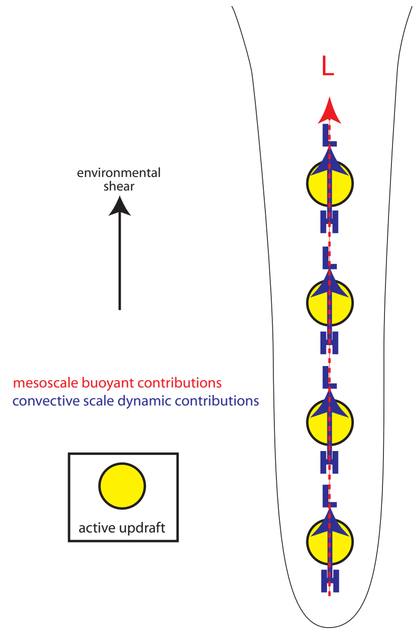

Figure 6: Conceptual model of a PS MCS depicting the convective–scale and mesoscale along–line pressure gradient accelerations. Pressure maxima and minima are indicated by "H" and "L" symbols. Pressure gradient accelerations are indicated by arrows. In both cases, the coloring denotes the nature of the feature. As explained in the text, the convective–scale accelerations predominate, but are largely lost when mesoscale spatial or temporal averaging is performed.

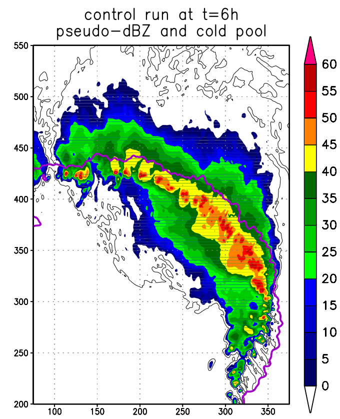

Figure 7: Same as Fig. 3a but for control PS MCS simulation at t=6h.

archetype for long periods of time without evolving toward TS structure. This is addressed further in Section 4.2.

4.2 Sensitivity tests

Part of the motivation for the present sensitivity experiments is that, in simulations with convective initiation by a warm bubble, new development tends to occur preferentially along the part of the cold pool that is orthogonal to the low–level shear vector. Because the base state includes comparable low–level shear in both the u and v components (Fig. 2), the control PS system in time tends to reorient itself toward a northwest–southeast line (Fig. 7). This is undesirable for an exploration of the dynamics of PS MCSs, because the upper level flow is no longer line–parallel. PS MCSs in the real world do not commonly evolve in this way because they tend to be triggered along pre–existing linear boundaries such as cold fronts (PJ00), which serve to maintain their orientation. However, initiating the convection with an infinitely long cold pool would remove the PS system's distinctly 3D character, and more complicated synoptic features are beyond the scope of the present, idealized study. Instead, by compartmentalizing the line–parallel shear to the layer above 3 km AGL (the "CS" profile; Fig. 2), it was possible to simulate convective lines that preserved their orientation with respect to the base state wind profile, and then to test their sensivity to the strength of the line–parallel and line–perpendicular shear.

With compartmentalized shear, the simulated convective system maintains its north–south orientation through the 6 hour simulation (Figs. 8b and 9b) and, although it evolves toward a TS/PS hybrid in time (Fig. 9b), it maintains a fairly archetypal PS structure through roughly t=4h (e.g. Fig. 8b). The CS run apparently resists the evolution toward TS structure somewhat longer than the control run because the low–level line–perpendicular shear has been increased (Fig. 2), providing for greater downshear accelerations of the low–level updraft air and hence more upright convective cells.

Increasing [decreasing] the upper–level line–parallel shear increases [decreases] the size of the line–parallel stratiform precipitation region, but on the whole does not impact the basic evolution of the CS run that much during the first few hours of simulation (cf. Figs. 8c,d). Differences become apparent, however, as time goes on. The CS–1.5xV_s simulation not only continues to have a larger PS region than does the CS–0.5xV_s simulation, but it is also narrower and has better resisted the seemingly inexorable march toward TS structure (Fig. 9c,d). These results are related: because in an environment with greater along–line shear, the convective system experiences larger along–line accelerations, a greater amount of the system's hydrometeor mass is advected away from the line into the PS region, and comparatively less falls in proximity to the pre–existing cold pool. Hence, the surface outflow is comparatively weaker in time for the CS–1.5xV_s simulation (roughly 5 K warmer than the CS run). This is one way that a PS MCS can persist for some time.

The impact of increasing or decreasing the low–level

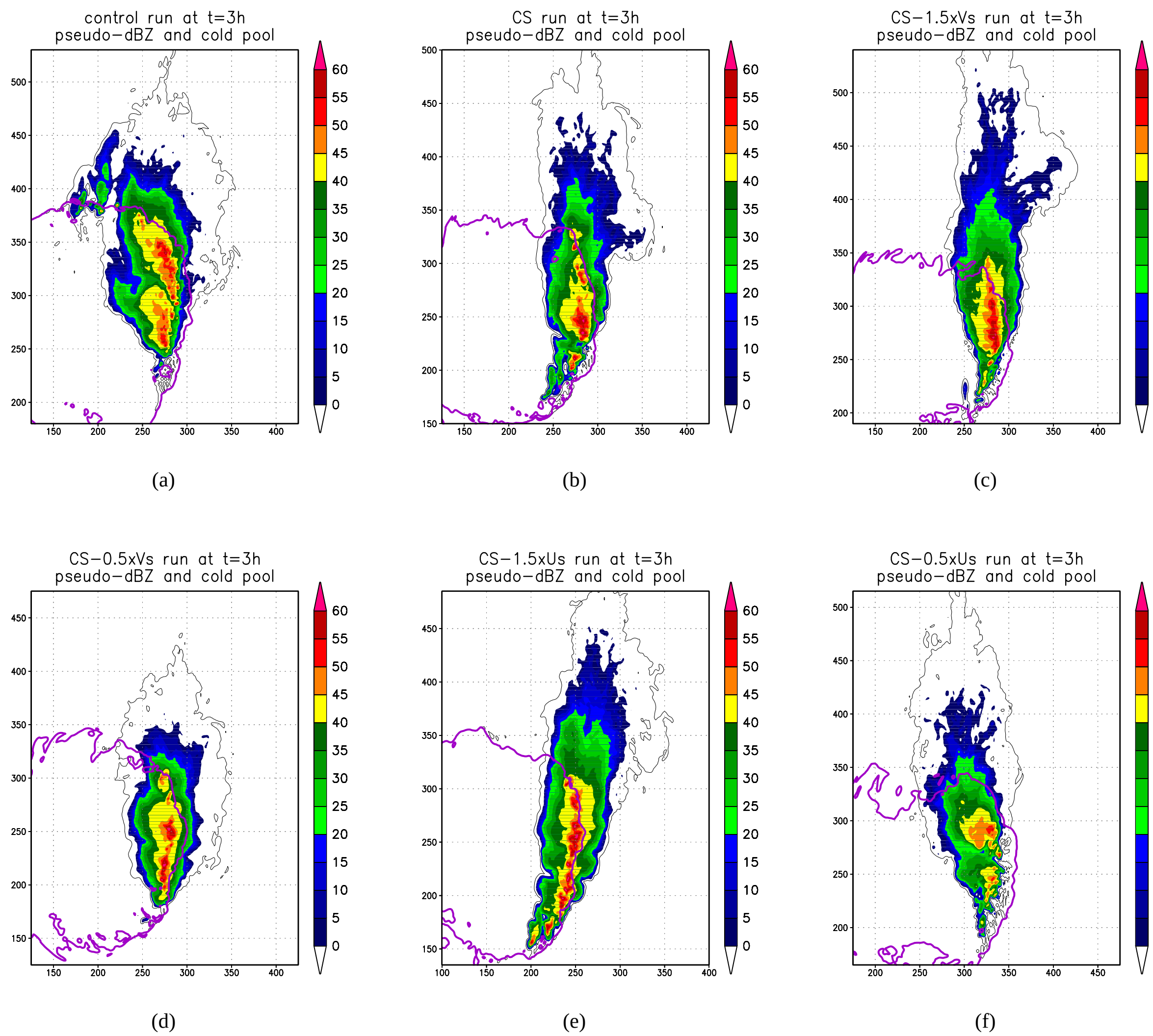

Figure 8: Same as Fig. 3a but for all six PS MCS simulations at t=3h. (a) control run, (b) CS run, (c) CS–1.5xV$_s$ run, (d) CS–0.5xV$_s$ run, (e) CS–1.5xU$_s$ run, (f) CS–0.5xU$_s$ run.

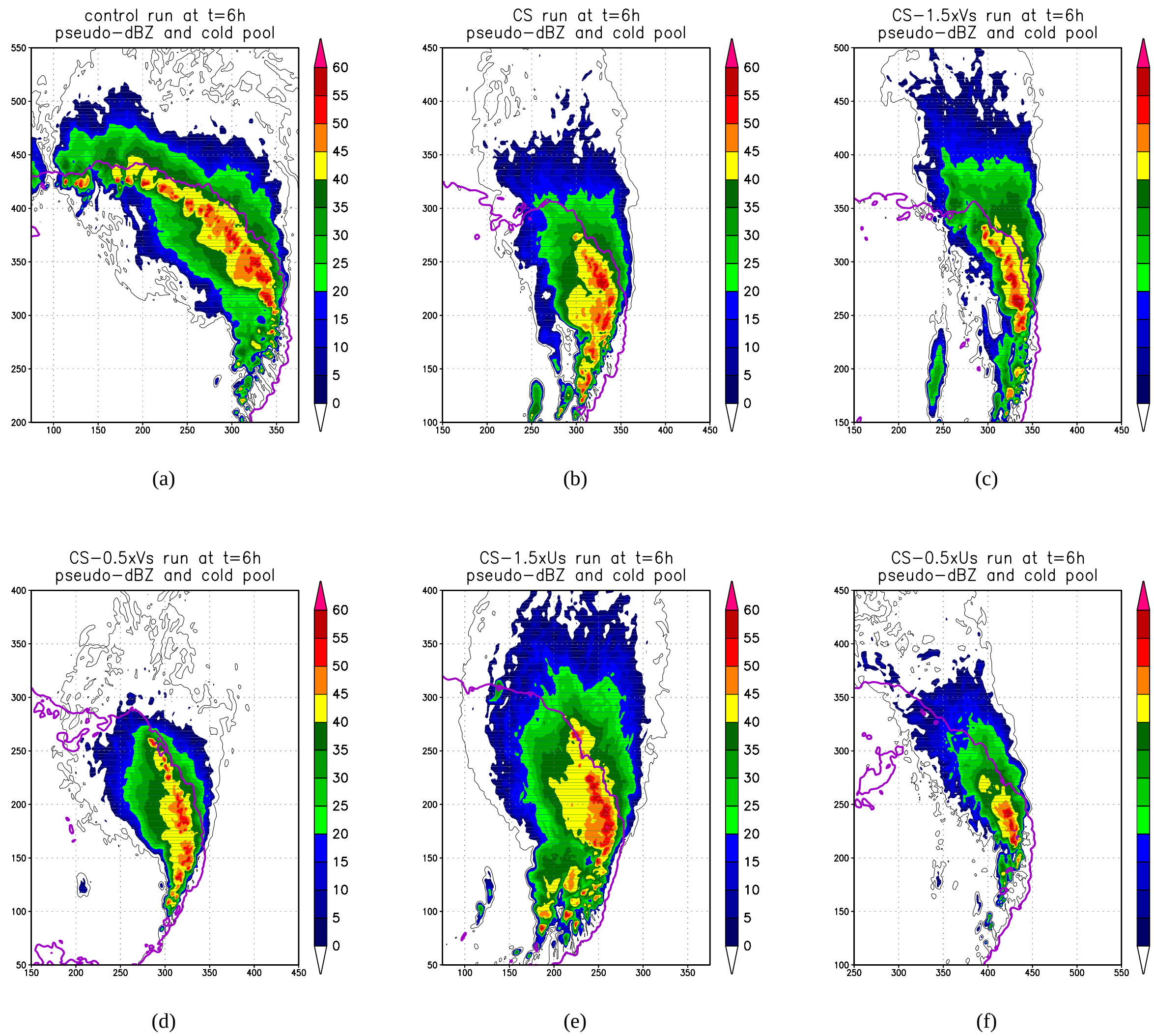

Figure 9: Same as Fig. 8a but for all six PS MCS simulations at t=6h.

line–perpendicular shear is also somewhat unique. As suggested by Rotunno et al. (1988), increasing the line–perpendicular shear toward an optimal condition renders a more intense, upright convective line. Thus, after 3 hours, the CS–1.5xU_s simulation has the strongest convection and most archetypal PS structure among all six cases (Fig. 8e). The along–line shear continues to render the parallel stratiform precipitation region. As described earlier, along–line advection tends to rapidly intensify the surface cold pool because most of the system's precipitation falls out in close proximity to the surface gust front. This is even moreso the case in the CS–1.5xU_s run, because the convective prectipiation is comparatively heavy and because the convective cores are directly above the outflow boundary (Fig. 8e). Ironically, the low–level shear that initially provides for a strong, upright convective line in time renders a large TS/PS hybrid (Fig. 9e), whose TS characteristics have come from the remarkable intensification of the outflow through this process. This simulation produced the strongest cold pool among all of the simulations: roughly 4 K colder than the control run and roughly 2 K colder than the CS run (not shown). Hence, increasing the low–level line–perpendicular shear beyond what is necessary for healthy convection appears, in the long run, to be less beneficial for the PS mode than does increasing the line–parallel shear. Decreasing the low–level line–perpendicular shear, as predicted by Rotunno et al. (1988), renders a relatively small, weak convective system that may be considered a TS/PS hybrid, although at times its appearance is barely linear (Figs. 8f and 9f). Hence, as suggested earlier, some moderate amount of low–level line–perpendicular shear is required for PS MCSs, in addition to the need for line–parallel shear throughout the troposphere.

It is also interesting to note that the TS/PS hybrids in Figs. 8 and 9 bear great resemblance to the asymmetric TS MCSs discussed by Loehrer and Johnson (1995) and Hilgendorf and Johnson (1998). Such asymmetric structures have often been attributed to the cumulative impacts of coriolis accelerations, or to the climatological distribution of high–θ_e air in the central United States. Neither of these explanations can be applied to the present idealized simulations, such that the behavior must be attributed to the wind profile. This may be yet another explanation for why the transition toward asymmetric MCS structures is so common. Any convective system that is initiated by a baroclinic zone, and parallel to it, will experience significant line–parallel wind shear provided that the vertical wind profile is in approximate thermal wind balance with the baroclinity. Perhaps the combination of line–perpendicular and line–parallel shear used in the present simulations is sufficiently common to account for some MCSs' commonly observed evolution toward asymmetry, much as suggested by Hilgendorf and Johnson (1998).

5. SYNTHESIS

Convective lines with parallel precipitation develop in environments with significant line–parallel tropospheric wind shear, but also require moderate line–perpendicular low–level shear. It is notable that many linear convective systems initiated along fronts will experience such wind profiles (provided the fronts are near thermal wind balance). Hence, PS systems are somewhat common to the midlatitudes (PJ00). In such situations, both backcuilding and line–parallel advection of hydrometeors combine to render the characteristic PS structure.

Notably, the along–line flow within the convective line is considerably weaker than that of the environment. The velocity of this air that has been processed by the convection, and not the environmental storm–relative flow, is actually responsible for the line–parallel transport of hydrometeors (and development of the PS region). The along–line flow within the line results largely from the downshear accelerations experienced by air that is ascending in the updrafts, even though this signal is lost when averages are computed over the entire convective system.

Because precipitation particles move primarily along their convective lines, PS systems produce most of their outflow in very close proximity to the surface outflow boundary. As a result, their cold pools may strengthen quite rapidly. Intensification of the outflow, along with the diminished line–parallel shear within the line, implies that such systems will commonly evolve toward a trailing precipitation structure in time. However, sensitivity tests suggest that situations with very large along–line shear may avoid this common transition.

MCSs' structures are largely determined by their interior flow fields, which in turn result from local accelerations within the convective system. Our ongoing work is directed toward analysis of updraft and downdraft trajectories in simulated PS systems, and to a more thorough explanation of the line–parallel and line–perpendicular accelerations.

REFERENCES

Doswell, C. A., III, H. E. Brooks, and R. A. Maddox, 1996: Flash flood forecasting: An ingredients–based methodology. *Wea. Forecasting*, **11**, 560–581.

Hilgendorf, E. R., and R. H. Johnson, 1998: A study of the evolution of mesoscale convective systems using WSR–88D data. *Wea. Forecasting*, **13**, 437–452.

LeMone, M. A., 1983: Momentum transport by a line of cumulonimbus. *J. Atmos. Sci.*, **51**, 281–305.

Loehrer, S. M., and R. H. Johnson, 1995: Surface pressure and precipitation life cycle characteristics of PRE-STORM mesoscale convective systems. *Mon. Wea. Rev.*, **123**, 600–621.

Parker, M. D., and R. H. Johnson, 2000: Organizational modes of midlatitude mesoscale convective systems. *Mon. Wea. Rev.*, **128**, 3413–3436.

Parker, M. D., and R. H. Johnson, 2004a: Simulated convective lines with leading precipitation. Part I: Governing dynamics. *J. Atmos. Sci.*, **61**, 1637–1655.

Parker, M. D., and R. H. Johnson, 2004b: Simulated convective lines with leading precipitation. Part II: Evolution and maintenance. *J. Atmos. Sci.*, **61**, 1656–1673.

Parker, M. D., and R. H. Johnson, 2004c: Structures and dynamics of quasi–2d mesoscale convective systems. *J. Atmos. Sci.*, **61**, 545–567.

Rotunno, R., J. B. Klemp, and M. L. Weisman, 1988: A theory for strong, long–lived squall lines. *J. Atmos. Sci.*, **45**, 463–485.

Schumacher, R. S., 2003: Climatological and radar–indicated characteristics of United States extreme rain events. M.S. thesis, Department of Atmospheric Science, Colorado State University, 143 pp. [Available from Department of Atmospheric Science, Colorado State University, Fort Collins, CO, 80523-1371.]

Szeto, K. K., and H.-R. Cho, 1994: A numerical investigation of squall lines. Part II: The mechanics of evolution. *J. Atmos. Sci.*, **51**, 425–433.

Xue, M., K. K. Droegemeier, and V. Wong, 2000: The Advanced Regional Prediction System (ARPS) - A multiscale nonhydrostatic atmospheric simulation and prediction tool. Part I: Model dynamics and verification. *Meteor. Atmos. Phys.*, **75**, 161–193.

Xue, M., K. K. Droegemeier, V. Wong, A. Shapiro, K. Brewster, F. Carr, D. Weber, Y. Liu, and D.-H. Wang, 2001: The Advanced Regional Prediction System (ARPS) - A multiscale nonhydrostatic atmospheric simulation and prediction tool. Part II: Model physics and applications. *Meteor. Atmos. Phys.*, **76**, 134–165.

ACKNOWLEDGMENTS

The research reported here is supported by the National Science Foundation under Grant ATM–0349069. The simulations in this study were made using the Advanced Regional Prediction System (ARPS) developed by the Center for Analysis and Prediction of Storms (CAPS), University of Oklahoma. These simulations were performed using the Research Computing Facility at the University of Nebraska–Lincoln, whose staff–members have been of great assistance.